

Guided Elastic Waves Produced by a Periodically Joined Interface in a Rock Mass

A.S. Yenwong Fai

School of Physics

University of the Witwatersrand

Johannesburg, South Africa

Email: alfred.yenwongfai@wits.ac.za

R.J. Durrheim

Mining Innovation CSIR, School of Geosciences

University of the Witwatersrand

Johannesburg, South Africa

Email: RDurrhei@csir.co.za

M.W. Hildyard

Department of Geophysics

University of Leeds

Leeds England

Email: M.Hildyard@leeds.ac.uk

Abstract—Mining-induced seismic events pose a serious risk to workers in deep mines. Accurate numerical simulations are useful in analyzing the problem and developing mitigation strategies. Here we tackle the problem of guided interfacial elastic wave propagation in a periodically joined interface of two half spaces. The problem is viewed as a mixed boundary-condition plane strain problem and a displacement discontinuity model is used to model the boundary condition. The coupled set of first order linear differential equations for stress and velocity for an elastic continuum are replaced by an explicit finite difference scheme that is implemented on a regular rectangular staggered grid. Phase velocity dispersion curves for the guided interfacial wave modes are obtained via a phase spectra analysis method. The analysis reveals that longer wavelengths travel faster than shorter ones and that the phase velocity dispersion curve is a function of many model parameters including: source type (shear or dilatation), source time function, inherent periodicity at the model interface and size of periodic strips joining the interface. Lastly, we observe that the medium acts like some sort of “soft” frequency filter.

Keywords—rockbursts; guided waves; dispersion; finite difference

I. INTRODUCTION

Rockbursts and rockfalls are serious hazards in deep hard-rock mines in South Africa and worldwide, posing significant risks to life, equipment and production [1]. An understanding of the types and nature of interfacial guided wave modes propagated in mine stopes can be of great benefit to the design of support structures in order to mitigate the effects of mining-induced seismic events. Motivated by the rockburst problem, we address here the problem of guided elastic waves at a periodically joined interface of two half spaces which can be viewed as an idealized stope environment.

Guided elastic waves at a periodically joined interface of two half spaces and other related problems have been addressed analytically by several authors in the continuum mechanics community including Every [2], Angel and Achenbach [3], Zhang [4] and Mikata [5]. Analytic solutions of these types of problems are considered to be very challenging, especially when modeled as a mixed boundary condition problem [1]. In particular, an analytic solution to the above problem framed as a 2D plane strain mixed boundary condition type problem (where two half spaces sharing a planar interface

are joined together within infinitely long regularly-spaced strips and unattached in between) has already been solved in the past via an elegant and efficient method of smoothing over discontinuities in the boundary conditions and invoking a Fourier series expansion of the scattered wave field; which results in a rich system of interfacial and pseudo-interfacial guided waves and supersonic interfacial waves [2].

The aforementioned problem is addressed here via a finite difference code called WAVE [1] [6], which solves a system of first order linear equations of stress and velocity via finite differencing on a regularly spaced orthogonal staggered rectangular grid; a method used frequently in seismological applications due to its computational efficiency. A displacement discontinuity is used in WAVE to model the mixed boundary condition at the interface. Phase velocity dispersion curves for the guided modes, resulting from the scattering of the fundamental bulk modes by the interface are obtained via a phase spectra analysis of time wave forms measured at different locations in the model [7].

We used two 2D plane strain linear elastic models for our investigations:

- A A homogeneous solid rock mass without an interface, serving as a control; and
- B Two half spaces having identical elastic properties separated by a periodically joined interface, the discontinuities and the joins representing stopes and pillars, respectively.

In general there is a modest visible difference in the dispersion for both models within the frequency range of 4 to 180 Hz, with little or no dispersion observed for the control model. Also, the general trend of the velocity dispersion curves reveals that lower frequencies travel faster than higher frequencies. It is also shown that the shapes of the dispersion curves are complexly dependent on the following model parameters including: periodicity of the structure, the ratio of the length of the periodic strips joining the interface to the periodicity of the structure, the type of seismic source (dilatational or shear), and the source time function introduced into the model. Also, a closer look at the amplitude spectrum of the spatial wave functions for the second model indicate that some frequencies undergo significant attenuation. This

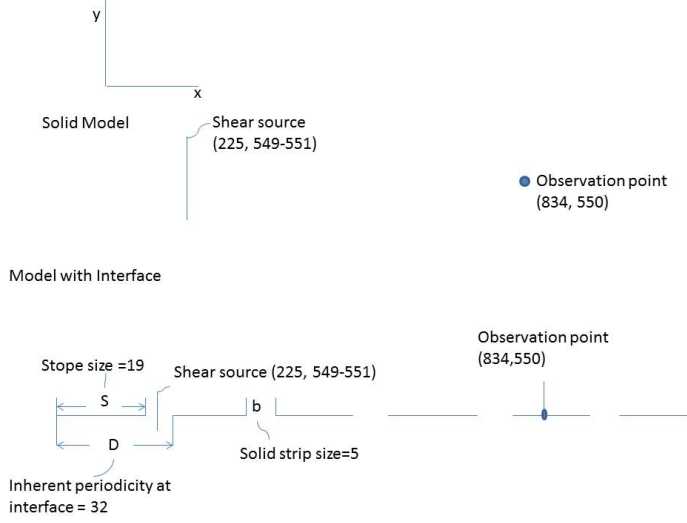


Fig. 1. Geometry of Models

could be due to destructive interference of such frequencies at the given positions, enabling the interface to act as some kind of “soft” frequency filter. It is worth mentioning that the dispersive behavior studied here is geometric dispersion which is a consequence of boundaries in the specimen [7].

The results obtained from the above 2D simplified model will serve as a basis for future 3D models with added complexities such as non-periodic discontinuities at the interface in order to be more representative of actual mining scenarios.

II. DESCRIPTION OF MODEL GEOMETRY

In this paper a plane strain assumption is made as in Every [2]. The physical models analyzed are depicted in Fig 1; which shows both a homogeneous linear elastic isotropic medium with a source (shear or dilatational) located at position (225, 550-551) and two identical homogeneous linear elastic isotropic half spaces which are periodically joined at their interface by infinitely long strips parallel to the z-axis and unattached in between. The strips and the unattached free portions of the interface each have widths of b and S respectively along the x-axis. The inherent periodicity at the interface in the x direction is D, as indicated in the figure (Where $D = b + S$).

III. THEORETICAL AND NUMERICAL BASIS FOR THE MODEL

Linear elasticity and isotropy is assumed. The governing equations of motions for the above mentioned system (neglecting the effect of body forces) are [1]:

$$\rho \frac{\partial \dot{u}_i}{\partial t} = \frac{\partial \sigma_{ij}}{\partial x_j} \quad (1)$$

where ρ is the density, and \dot{u} is the velocity. Since the system is elastic and linear, the stress and strains components are related by the following constitutive equations:

$$\sigma_{ij} = \delta_{ij} \left(K - \frac{2}{3}G \right) e_{kk} + 2Ge_{ij} \quad (2)$$

where K and G are the shear and bulk moduli respectively, δ_{ij} is the Kronecker delta, $e_{ij} = \frac{1}{2} \left[\frac{\partial u_i}{\partial x_j} + \frac{\partial u_j}{\partial x_i} \right]$ are components of the strain tensor, and σ_{ij} are components of the stress tensor.

Differentiating 2 we obtain the following equation; relating stress and velocity:

$$\dot{\sigma}_{ij} = \delta_{ij} \left(K - \frac{2}{3}G \right) \dot{e}_{kk} + 2G\dot{e}_{ij} \quad (3)$$

Equations 1 and 3 form a set of coupled equation of stress and velocity.

The above first order coupled differential equations of stress and velocity are solved using a code called WAVE [6] which solves the coupled system via an explicit time marching finite difference scheme implemented on a regular orthogonal staggered grid, whereby the grid variables of stress and velocity are updated at different points in time and space. This approach is generally efficient with respect to the use of computer resources such as memory and run time and is frequently used in seismological applications for example [8] and [9]. The grid equations used in WAVE can be found in [1].

A displacement discontinuity is used in WAVE to model the mixed boundary condition at the interface [1]. Dynamic motion in this paper is introduced via active sources (dilatation or shear), which are prescribed space-time distributions of stress in the model, thus representing approximately an explosion or a slip on a fault.

Phase velocity dispersion curves for guided modes, resulting from the scattering of the fundamental bulk modes by the interface, are obtained via an analysis of phase spectra time wave forms measured at two different locations in the model [7]. The equation for the above procedure is given as follows:

$$v(f) = \frac{2\pi fL}{\phi_i(f) - \phi_o(f)} \quad (4)$$

IV. SPECIFICATION OF PARAMETERS USED IN THE MODEL

A 2D grid of 1800×1800 elements of size $2m \times 2m$ (i.e. $dx=2m=dy$) is generated. A *rha* and an *rfull* (adaptations of the Ricker wavelet)[Mark Hildyard personal communication] source time functions (pulses) are applied to the stresses σ_{11} and σ_{22} (for the dilatational source), which generates symmetric particle displacement modes with respect to the interface and applied to σ_{12} (for the shear source), which results in the propagation of anti-symmetric modes [2].

The pulse duration was chosen to be $T=2.14$ s, 2.19 s, 2.8 s; so that pulse components with largest amplitudes are those for which their \vec{k} vector is in an $\epsilon=0.5$ neighborhood of the Brillouin-zone boundary in the k_x space (i.e. $k_x D \simeq 1$) [2]. T also satisfies the criterion necessary for stability of the finite difference scheme and to minimize numerical dispersion, a common feature of finite difference methods [9] and [10]. Stope sizes used are $S = 13, 27, 54$ grid spacings; solid strip

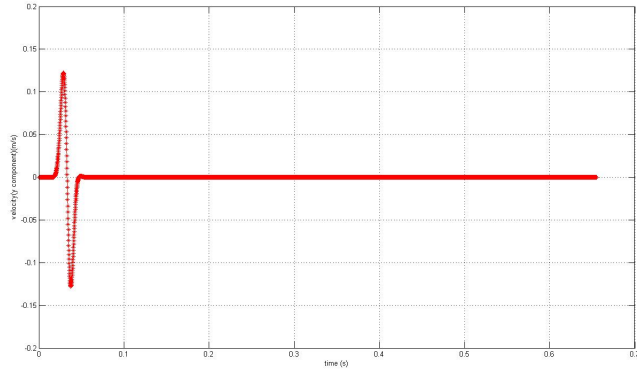


Fig. 2. Excited pulse in model A

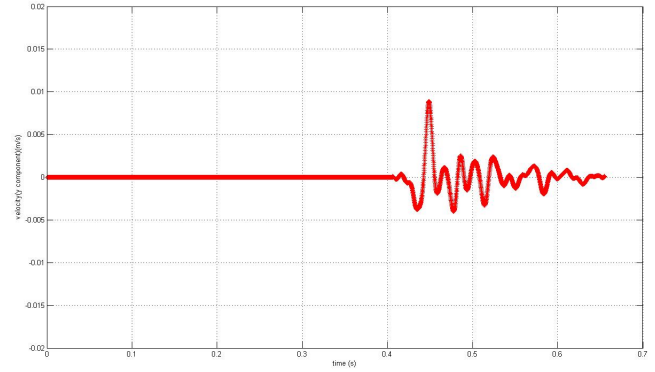


Fig. 5. Received pulse in model B

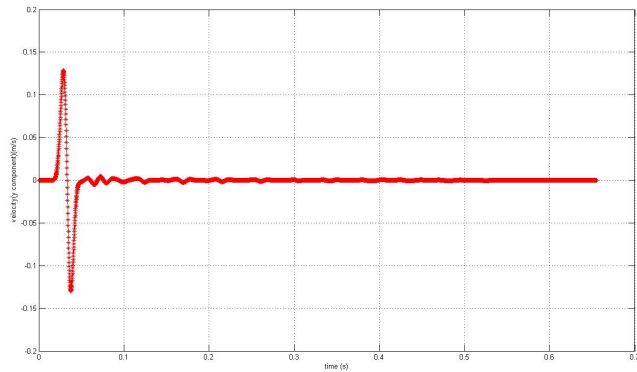


Fig. 3. Excited pulse in model B

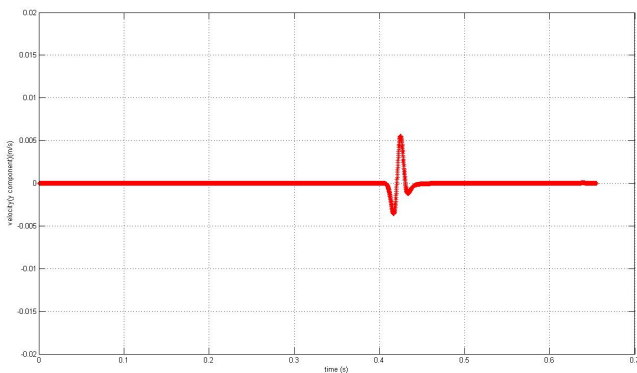


Fig. 4. Received pulse in model A

V. RESULTS AND DISCUSSIONS

Figures 2 and 3 shows the y-component of the velocity resulting from the excited shear pulse at grid points (225, 549-551) ($x=450$ m from boundary and length of source in the y direction is 3 m) for both the models A and B. The pulse duration used is $T=2.19$ s; containing mostly frequency components in the interval 4 to 180 Hz. Here $S=27$ and $b=5$; so that the ratio of $b/D=0.16$ as in Every [2]. Figs. 4 and 5 show the received pulse at grid location (810, 550) after propagation through the mediums in models A and B. The P-wave part of the received pulse in model B was removed because it was very small in magnitude compared to the S-wave portion shown and was somewhat indistinguishable from numerical noise. The received pulses have a negative first motion polarity with respect to the pulse at the source. This happens so that linear momentum can be conserved since points on the left of the source (not shown in the figure) have a positive first motion polarity. It is clear from these figures that there is little or no observable distortion (except for the first motion polarity reversal as described above) in the received pulse in model A, while there is significant distortion for the received pulse in model B.

Using the above data and equation 4, we calculate the phase velocity for model A and B and the results are displayed in Fig. 6. There is clearly a visible difference in the dispersion curves displayed in Fig. 6, showing that different modes are being propagated in the mediums. Also, there is no significant difference in the value of the magnitude of the phase velocity for both modes (with one being about 5 percent more than the other) which is similar to observations made in [2] for anti-symmetric modes. The overall pattern in the dispersion curves corresponds to what is expected in the literature with respect to geometric dispersion [11] where lower frequencies on average, travel faster than higher frequencies. Also, we observe that the phase velocities asymptotically approach infinity for small frequencies corresponding to the mode cutoff frequency.

The phase velocity frequency variation of the mode in model A is very gradual beyond the cutoff frequency, which should be

sizes $b = 5, 10, 19$ grid spacings. The corresponding inherent periodicity sizes for appropriate combinations of S and b is easily obtained from $D = S + b$.

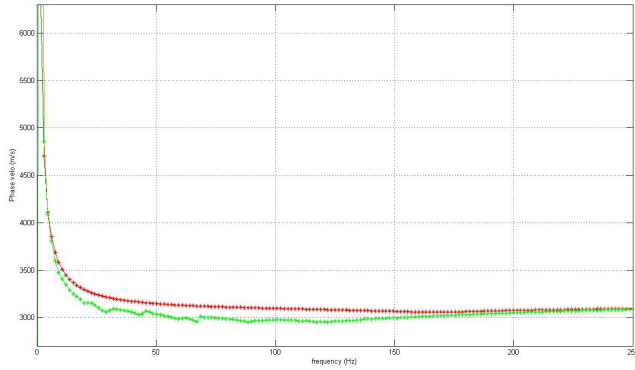


Fig. 6. Phase velocities for models A (red) and B (green)

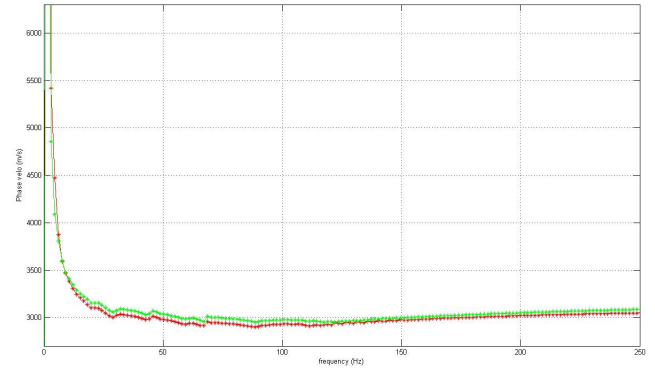


Fig. 8. Effect of change in pulse duration; $T=2.8$ s (red) and for $T=2.19$ s (green) in model B

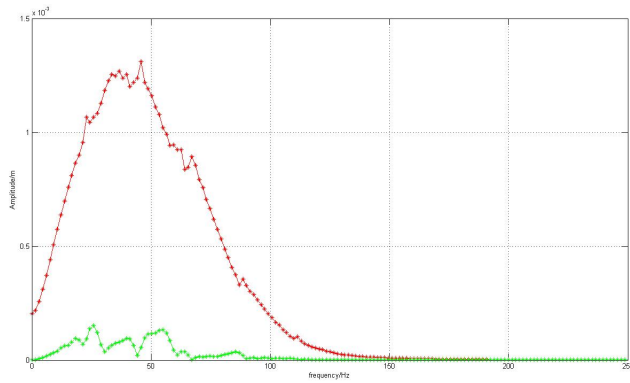


Fig. 7. Amplitude spectrum at the source (in red) and receiver (in green) position in model B

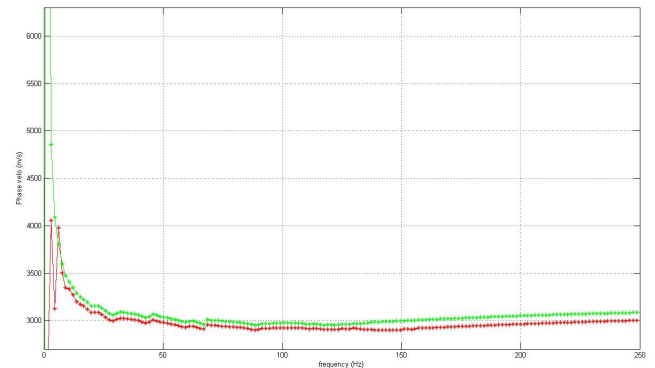


Fig. 9. Effect of change in pulse type; *rfull* (red) and *rha* (green) source time functions in model B

expected since it is the bulk shear wave mode which is being propagated. Its value is not exactly 3000 m/s but about 3150 m/s which is 5 percent more than 3000 m/s. This difference is due to numerical errors associated with the coarse grid used. In the case of model B, the phase velocity of the propagated mode follows a much less gradual frequency variation compared to the mode in A and seems to asymptotically approach the phase velocity value of the shear wave mode in A.

Fig. 7 shows the amplitude spectrum of the pulse at the source position in red and receiver position in green. There is a significant attenuation of the amplitudes at the receiver position, which is largely due to geometric spreading. Moreover, the relative frequency amplitudes in the signal at the receiver position is very different from that at the source position indicating that certain frequencies undergo more attenuation than others. This phenomenon may be due to destructive interference of certain frequencies at given positions in the medium, and possibly a slight constructive interference of other frequencies thus enabling the interface to act as a “soft” frequency filter.

Figs. 8, 9, 10 and 11 displays the phase velocity dispersion curves for model B in which the following model parameters

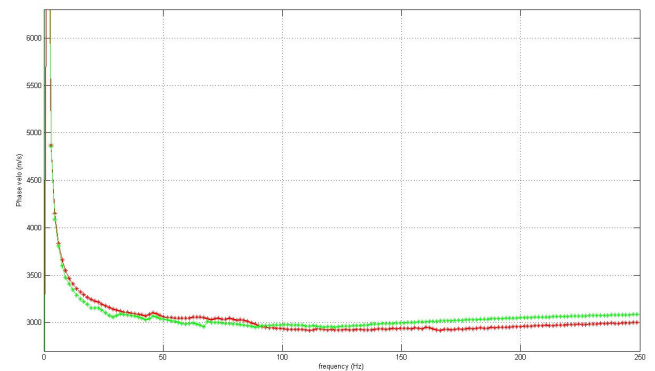


Fig. 10. Effect of change in structure at interface; $b=19$ and $S=13$ (red) and $b=5$ and $S=27$ in (green) in model B

where altered. For the shear source used in model B above the following alterations were done: the pulse duration change to $T=2.8$ s, the source time function *rfull* was used, the size of the strip, $b=19$ and free space $S=13$ and finally, the periodicity of the structure $D=64$ grid spacings ($S=54$ and

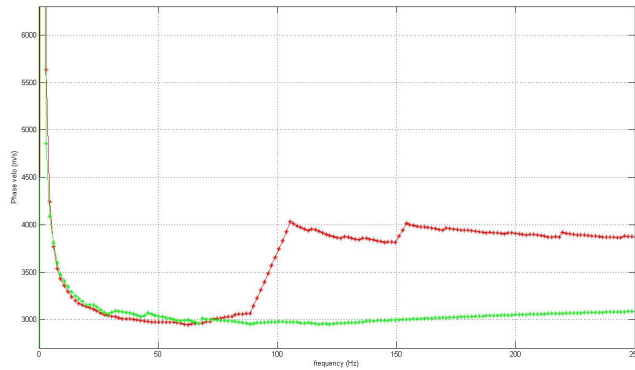


Fig. 11. Effect of change in structure periodicity; D=64 (red) and D=32 (green) in model B

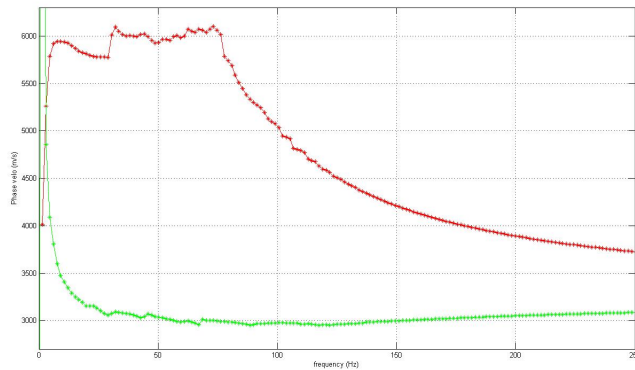


Fig. 12. Effect of change in source type; dilational source (red) and a shear source (green) in model B

b=10). A dilatational source was then used in model B above with $T=2.14$ s. The resulting phase velocity for P-wave phase of the disturbance is depicted in Fig. 12. The phase velocity at low frequencies (10–100 Hz) varies somewhat erratically within the velocity interval [5750, 6200]m/s. This is to be expected as the P-wave velocity for the solid model is 6250 m/s.

The above investigations were done in order to determine how sensitive the phase velocity dispersion curve is to the aforementioned model parameters. The Figures above show that the dispersion curves for the phase velocity are dependent on the above mentioned model parameters. Thus, indicating that these model parameters play a crucial role in the nature and type of interfacial modes propagated at the interface of the system.

VI. CONCLUSION

A finite difference method coupled with a phase spectra analysis method have been used to obtain phase velocity dispersion curves for a mixed boundary conditioned-type problem involving two linear elastic half spaces which are periodically joined at their interfaces. We have also demonstrated that

the nature and type of the interfacial waves propagated is influenced by the following model parameters including type of seismic source (shear or dilatation), the source time function introduced into the model, the pulse width, the periodicity of the structure, the ratio of the length of the periodic strip joining the interface to the periodicity of the structure. The amplitude spectrum of the transmitted pulse also reveals that certain frequencies are significantly attenuated relative to others enabling the interface to behave like a “soft” frequency filter. The results obtained in this work will serve as a basis for future 3D models with added complexities such as non-periodic discontinuities at the interface in order to be more representative of real life mining scenarios. Also, a further study of the amplitude spectrum with respect to the attenuation or enhancement of certain frequencies in the signal could reveal useful information about possible resonances in a mine stope [12].

REFERENCES

- [1] M. Hildyard, “Wave interaction with underground openings in fractured rock,” Ph.D. dissertation, University of Liverpool, September 2001.
- [2] A. Every, “Guided elastic waves at a periodic array of thin coplanar cavities in a solid,” *Physical Review B*, vol. 78, p. 174104(11), November 2008.
- [3] Y. Angel and J. Achenbach, “Reflection and transmission of elastic waves by a periodic array of cracks: Oblique incidence,” *Wave Motion*, vol. 7, pp. 375–397, 1985.
- [4] C. Zhang, “Reflection and transmission of sh wave by a periodic array of interface cracks,” *International Journal of Engineering Science*, vol. 29, no. 4, pp. 481–491, 1991.
- [5] Y. Mikata, “Reflection and transmission by a periodic array of coplanar cracks: Normal and oblique incidence,” *ASME Trans. J. Appl. Mech.*, vol. 60, no. 4, p. 911 (9pages), 1993.
- [6] M. Hildyard and R. Young, “Modelling seismic waves around underground openings in fractured rock,” *Pure and Applied Geophysics*, vol. 159, pp. 247–276, 2002.
- [7] S. Wolfgang and A. Yih-Hsing P, “On the determination of phase and group velocities of dispersive waves in solids,” *Journal of Applied Physics*, vol. 49, no. 8, pp. 4320–4327, August 1978.
- [8] M. Hildyard, “Wave interaction with underground openings in fractured rock,” *Rock Mechanics and Rock Engineering*, vol. 40, pp. 531–561, October 2007.
- [9] R. W. Graves, “Simulating seismic wave propagation in 3d elastic media using staggered grid finite differences,” *Bulletin of Seismological Society of America*, vol. 86, no. 4, pp. 1091–1106, August 1996.
- [10] J. Virieux, “P-sv wave propagation in heterogeneous media: velocity-stress finite difference method,” *Geophysics*, vol. 51, no. 4, pp. 1091–1106, April 1986.
- [11] L. R. Joseph, *Ultrasonic waves in Solid Media*, 1st ed. Cambridge University Press, 1999.
- [12] A. Cichowicz, A. Milev, and R. Durrheim, “Rock mass behaviour under seismic loading in a deep mine environment: implications for stope support,” *The Journal of the South African Institute of Mining and Metallurgy*, no. 121-128, p. April, 2000.